Age-dependent involvement of gut mast cells and histamine in post-stroke inflammation

Maria Pilar Blasco
University of Texas Health Science Center at Houston
Anjali Chauhan
University of Texas Health Science Center at Houston
Pedram Honarpisheh
University of Texas Health Science Center at Houston
Hilda Ahnstedt
University of Texas Health Science Center at Houston
John d'Aigle
University of Texas Health Science Center at Houston
Arunkumar Ganesan
Baylor College of Medicine
Sriram Ayyaswamy
Baylor College of Medicine
Frank Blixt
University of Texas Health Science Center at Houston
Susan Venable
Baylor college of medicine
Angela Major
Baylor college of medicine
David Durgan
Baylor college of medicine
Anthony Haag
Baylor College of Medicine
Julia Kofler
University of Pittsburgh
Robert Bryan
Baylor College of Medicine
Louise D McCullough
University of Texas Health Science Center at Houston
Bhanu Priya Ganesh (Bhanu.P.Ganesh@uth.tmc.edu)
University of Texas Health Science Center at Houston https://orcid.org/0000-0003-1575-7914

Research

Keywords: Mast cells, Histamine, Histamine receptor, Cytokines, post-stroke, microbiome, intestinal epithelium

Posted Date: March 24th, 2020

DOI: https://doi.org/10.21203/rs.2.21718/v2

Version of Record: A version of this preprint was published at Journal of Neuroinflammation on May 19th, 2020. See the published version at https://doi.org/10.1186/s12974-020-01833-1.

Abstract

Background Risk of stroke-related morbidity and mortality increases significantly with age. Aging is associated with chronic, low-grade inflammation, which is thought to contribute to the poorer outcomes after stroke seen in the elderly. Histamine (HA) is a major molecular mediator of inflammation and mast cells residing in the gut are a primary source of histamine. Methods Stroke was induced in male C57BL/6J mice at 3 months (young) and 20 months (aged) of age. Role of histamine after stroke was examined using young (Yg) and aged (Ag) mice, mice underwent MCAO surgery and were euthanized at 6h, 24h and 7 days post-ischemia; sham mice received the same surgery but no MCAO. In this work, we evaluated whether worsened outcomes after experimental stroke in aged mice was associated with age-related changes in mast cells, histamine levels, and histamine receptor expression in the gut, brain, and plasma. Results We found increased numbers of mast cells in the gut and the brain with aging. Using the middle cerebral artery occlusion (MCAO) model of ischemic stroke, we demonstrate that stroke leads to increased numbers of mast cells and histamine receptors in the gut. These gut-centric changes are associated with elevated levels of HA and other pro-inflammatory cytokines including IL-6, G-CSF, TNF-α, and IFN-γ in the peripheral circulation. Our data also shows that post-stroke gut inflammation led to a significant reduction of mucin-producing goblet cells and a loss of gut barrier integrity. Lastly, gut inflammation after stroke is associated with changes in the composition of the gut microbiota as early as 24 hours post-stroke. Conclusion An important theme emerging from our results is that acute inflammatory events following ischemic insults in the brain persist longer in the aged mice when compared to younger animals. Taken together, our findings implicate mast cell activation and histamine signaling as a part of peripheral inflammatory response after ischemic stroke, which are profound in aged animals. Interfering with histamine signaling orally might provide translational value to improve stroke outcome.

Introduction

Aging is a major risk factor for stroke, stroke-related mortality, and post-stroke complications [1]. Aging is associated with increased inflammation and changes in the immune response to injury [2, 3]. To date, few studies have investigated the effects of aging on peripheral immune responses after ischemic stroke. Histamine (HA) is a major mediator of acute inflammatory response to tissue injury [4-7] . Among HA-producing cells, mast cells (MCs) are a major source of HA in the early phases of inflammation [8-10] [11]. MCs release stored and newly synthesized HA along with other inflammatory mediators such as proteases, cytokines and chemokines [9, 12-17]. As the largest immune organ in the body, the gut is a major site of MC progenitors and HA production [18, 19]. Gut MC progenitors constitutively home to the intestinal mucosa [20, 21], and upon initiation of the inflammatory response, they are recruited out of the gut environment and mature in a HA-dependent manner [15]. The inflammatory cascade originating in the cerebral vasculature that leads to the systemic immune response by brain ischemia is a major factor in stroke pathophysiology and outcome [22-24].

Accumulating pre-clinical data suggests that stroke leads to a more significant disruption of gut homeostasis in aged mice when compared to young mice [25, 26], but the molecular mediators of these age-dependent changes are poorly defined. MCs are among the first-responders to tissue injury and secrete large amounts of HA to initiate a cascade of local and systemic inflammatory processes [11]. The diverse effects of HA are determined by the function, structure, tissue distribution, and ligand affinity of the four HA receptor subtypes (H1R through H4R) [8] [27]. In the gut, the majority of HA receptors are of H1R and H2R subtypes [28, 29].

Using global MC knockout models, one study reported that meningeal MCs worsen stroke-induced brain injury in murine models [30]. Given the limitation of global knockout models however, the role of gut MCs, HA and HA receptors, where most progenitor MCs are found [19, 31], has not been evaluated after stroke. We hypothesized that in aged mice, stroke would induce enhanced peripheral inflammation, and an increase in MCs and HA receptor activation in the gut. Therefore, we aim to examine peripheral gut mast cell activation and histamine signaling in response to stroke. Aged MCs are known to be in an increased state of activation [32]. In this work, we evaluated age-dependent changes in local and systemic HA levels, HA receptors, and gut MCs after stroke. Specifically, we investigated how the gut HA and HA receptor levels differ in response to stroke at 6 hours, 24 hours and 7 days after experimental stroke and compared the response in young (Yg) and aged (Ag) mice. We found that MCs increase with age in both the gut and in the brain. Our data also showed that H2R expression, loss of gut barrier integrity, and elevated plasma HA and other pro-inflammatory cytokines after stroke persist significantly longer in aged mice, when compared to young mice. Gut MCs increased at 24 hours and 7 days after stroke in aged but not in young mice. Lastly, these changes in HA and MCs in the gut were associated with a shift in bacterial phylum and changes in the beta- (between groups) diversity of the gut microbiota in aged mice when pre-stroke gut luminal samples were compared to post-stroke samples. Together our results suggest that age-dependent differences in HA signaling and gut MCs contributes to the response to stroke. Pharmacological intervention of MC degranulation or inhibition of the HA-mediated inflammatory cascade might be promising therapy to dampen the prolonged phase of inflammation seen with aging.

Materials And Methods

Animal experiments:

C57BL/6J young (3-months) and aged (20 months) male mice were housed in a specific pathogen-free facility (light cycle 12/12 h light/dark). Food and water were provided ad libitum. Due to changes in estrous cycle that has impact on histamine levels in young females[33], we used only males for this study.

Experimental groups

To examine the role of histamine after stroke in young (Yg) and aged (Ag) mice, mice underwent MCAO surgery and were euthanized at 6h (n=5), 24h (n=5) and 7 days (n=5) post-ischemia; sham mice received the same surgery but the suture was not inserted into the MCA (n=3,5). In total, the groups were divided

into Yg-6-sham, Yg-6-stroke, Yg-24-sham, Yg-24-stroke, Ag-6-sham, Ag-6-stroke, Ag-24-sham and Ag-24-stroke. Seven-day post-ischemic studies were performed only in aged mice (Ag-7d-Sham and Ag-7d-Stroke). A mortality of 20% was observed in the aged 24 hours MCAo cohort additionally, 40% mortality was seen at 7 days in aged MCAo mice.

Middle cerebral artery occlusion (MCAo)

Animals in the respective groups underwent transient focal ischemia under isoflurane anesthesia for 1 hour by occlusion of the right middle cerebral artery (MCA). Body temperature was maintained at 37.0 ± 1.0°C throughout the surgery by an automated temperature control feedback system. One hour after MCAo, animals were re-anesthetized and reperfusion was established by the withdrawal of the monofilament. Animals were placed in a recovery cage. All mice were given subcutaneous injections of 0.9% sodium chloride twice a day for 7 days and were provided with wet mash in their cages. Body weight was recorded daily for the duration of the experiments. All experiments were performed by investigators blinded to animal groups and treatments to reduce experimenter bias.

Immunohistochemistry:

Formalin fixed, paraffin-embedded intestinal (cecal, ileum) tissue sections (4 µm) were incubated overnight at 4 °C with a primary antibody targeting the mouse antigens 1) histamine receptor 2 (AHR-002, Alomone labs, Israel), 2) Tryptase (ab2378, Abcam, USA), after antigen retrieval according to the manufacturer's instructions. Samples were washed and subsequently incubated with secondary antibody for 45 min at RT (Histofine simple stain anti-rabbit, 414341F, Nacalai, USA and Alexa fluor® 647, ab150131, Abcam, USA). Sections were counter-stained either with the diaminobenzidine substrate kit (Nacalai, USA) followed by haematoxylin or sections were stained with 6-diamidino-2-phenylindole (DAPI, Thermofischer, USA) as previously described for visualization of cell nuclei.

Lectin staining to visualize intestinal mucus secreting goblet cells:

Mouse cecal segments were fixed in Carnoy's fixative, embedded in paraffin and serially sectioned to 5 mm sections. Section were stained with hematoxylin and eosin (H&E) for intestine architecture. Terminal mucin glycans were examined using a panel of FITC-conjugated lectins: *Ulex europaeus* agglutinin-1 (UEA-1) for terminal fucose; concanavalin A (CONA) for mannose, *Dolichos biflorus* agglutinin (DBA) for N-acetylgalactosamine, Peanut agglutinin (PNA) for galactose and Wheat Germ Agglutinin (WGA) for N-acetylglucosamine (Vector Laboratories, Burlingame, CA) as previously described [34]. Briefly, de-paraffinized sections were incubated with citrate buffer pH 6 (Vector Labs) for 20 min in a pressure cooker and blocked with PBS containing 10% BSA. Sections were then stained in a humidified chamber with FITC-labeled lectin (10 mg/ml) for 1 h at room temperature. Sections were washed with PBS, counterstained with DAPI (Thermo Fischer, USA) for 5 min at room temperature and mounted using aqueous mounting media (Sigma Aldrich). Sections were analyzed by confocal microscopy (Leica Dmi8) and fluorescence was semi-qualitatively calculated by tabulating mean pixel intensity using ImageJ software (National Institutes of Health).

mRNA in-situ hybridization of intestinal tissues:

mRNA in situ hybridization (ISH) was performed on the distal ileum part of intestinal tissue from the sham and stroke cohort by using the RNAscope 2.5 HD assay system (Advanced Cell Diagnostics, Hayward, CA) with recommended probes [Probe-Mm-Hrh1 (Catalogue # 491141), Probe-Mm-Hrh2 (catalogue # 517751), RNAscope 2.5 HD reagent kit-Red]. ISH scores were generated at ×200 magnification and recorded using the RNAscope system Counting guidelines: number of purple dots (positive stain for H2R mRNA) per villi. Each point represents data from 15 crypts per section per sample.

Fluorescence in situ hybridization (FISH)

For intestinal tissue preparation, the small and large intestines were carefully removed immediately following euthanasia and rapidly dissected. Mouse terminal ileum (3-6 cm above the cecum), cecum, and mouse proximal and distal colon were carefully removed, fixed in 10% formalin fixative at room temperature for 24 hours followed by 70% ethanol transfer, then rinsed in 100% ethanol and embedded in paraffin wax. The tissues were sectioned at a thickness of 4 µm. These sectioned tissues were used for FISH staining as described. Four µm sections were mounted on glass slides, baked at 60°C for 1 hour, then de-paraffinized with xylene and dehydrated in 100% ethanol followed by incubation in ddH2O. A previously validated, 5' Cy3'-labelled, *EUB*338 bacteria-specific probe (Bact338; 5'-GCTGCCTCCCGTAGGAGT-3') which is complimentary to the V1 to V4 region of the 16S rRNA gene that is highly conserved in bacteria domain. The probe was hybridized to the samples by adding 20-25 µL of 1:25 dilution probe with hybridization buffer to each slide and placed in a hybridization chamber at 51°C for overnight. Nuclei were labeled with DAPI. Intestinal sections from mice in each cage (total 5-6 per group) were utilized to confirm bacterial location. The slides were analyzed using a Leica DMi8 confocal microscope (Leica biosystems, USA) equipped with appropriate filter set for Cy3' fluorescence (ex 550nm / em 570 nm).

Intestinal content collection and 16S rRNA gene sequencing:

Microbiota in the intestinal (cecum and feces) samples, were collected from mice and stored in sterile tubes at -80°C until analyzed. Bacteria taxa in each intestinal content samples were analyzed by amplifying the V4-V5 hyper-variable regions of the 16S rRNA gene using high throughput sequence analysis (Illumina MisSeq platform). Quality filtered 16S rRNA sequences were clustered into operational taxonomic units (OTU's), with 97% similarity, by closed reference OTU-picking using the UCLUST algorithm and GreenGenes reference database (v13.5) as implemented in Quantitative Insights Into Microbial Ecology (QIIME versions 1.6 and 1.7). Sequences were checked for chimeras using ChimeraSlayer with standard options as implemented in QIIME. Sequences not clustered were identified using the Ribosomal Database Project to the lowest possible taxonomic level. The data were randomly rarefied to 10,000 sequences per sample prior to any downstream analysis.

Murine cytokine measurements in blood plasma by protein multiplex:

Relative amounts of GM-CSF, IFN-gamma, IL-1, IL-6, IL-9, IP-10/CXCL10, MCP-1/CCL2, VEGF-A and G-CSF in the blood plasma were measured using cytokine multiplex kits (Millipore, Billerica, MA, USA). Quantification of cytokines was performed using the MAGPIX system (Austin, TX, USA) according to the manufacturer's instructions. Briefly, 25 µl of plasma samples collected from each mouse were thawed completely and diluted with the same amount of Assay Buffer provided in the kits. The assays were performed in duplicate blindly. The reports generated by MILLIPLEX® Analyst 5.1 Software were carefully reviewed and only cytokines that were within the limit of detection value and below the saturated value were considered. The detection limits for the aforementioned cytokines were between 10,000 pg/ml and 3.20 pg/ml, respectively.

mRNA gene expression in the intestinal mucosa:

To quantify relative mRNA expression levels of Histamine receptor 1 and 2 (H1R and H2R), interferon (IFN)-γ, tumor necrosis factor (TNF)-α, interferon gamma-inducible protein (IP)-10, interleukin (IL)-6, IL-1 and IL-12, RNA was extracted from intestinal mucosa samples (cecum) using the miRNeasy® mini kit (QIAGEN). One µg of RNA was reverse-transcribed to single-stranded cDNA using the RevertAid H minus First Strand cDNA Synthesis Kit (Thermo Fischer, USA). Reverse transcriptase real-time (RT) PCR was performed using the Quant Studio 3 Real-Time PCR system (Applied Biosystems, USA). The RT-PCR reaction mix (adjusted with H_2O to a total volume of 20 µl) contained 1 µl template DNA, 10 µl Power SYBR Green PCR master mix (ABI), 0.5 µl of the respective primers (10 µM each). The forward and reverse primers used for IFN-γ, IP-10, IL-12, IL-17, TNF-α, and IL-6 quantification were described previously [5, 35]. Relative mRNA target gene expression levels (Ratio = $[(E_{target})^{dCPtarget\ (control-sample)}]$ / $[(E_{ref.})^{dCPref.\ (control-sample)}]$) were normalized to the house keeping gene glyceraldehyde 3-phosphate dehydrogenase (GAPDH) and used as a reference. Subsequently, intestinal mucosal cytokine of the sham control group were set to 1.0 and used as the calibrator to identify the relative mRNA fold difference between the sham and stroke groups at 6 hours, 24 hours and 7 days after stroke.

Toluidine blue staining in human autopsy brain:

Formalin fixed paraffin embedded human brain autopsy sections were cut at 30µm. The slides were deparafinnized and hydrated. Slides were treated with Toluidine blue working solution (1% Toluidine blue ethanol solution in 1% sodium chloride) followed by dehydration. Nuclei were counterstained with hematoxylin. Human brain autopsy samples were obtained from stroke patients. The infarct region is from the cortex. MCs were quantified by counting the positively stained cells around the infarct region per section with a 40X magnification.

Flow cytometry:

Brain: After removal of intestinal tissue, mice were transcardially perfused with 60 ml cold, sterile PBS prior to aseptic removal of spleen, lung, and brain tissues. Brain tissue was placed in complete Roswell Park Memorial Institute medium 1640 (Lonza) medium and mechanically and enzymatically digested in

Collagenase/Dispase (1 mg/mL) and DNase (10 mg/mL; Roche Diagnostics) for 45 minutes at 37 °C. Lung tissue was processed similarly with the exception that digestion cocktail contained hyaluronidase (MilliporeSigma, 3000U/digestion), as well. The cell suspension was filtered through a 70 µm filter. Leukocytes were harvested from the interphase of a 70%-to-30% and 70%-to-40% Percoll gradients for the brain and the lung tissues, respectively. MCs were gated for CD45 positive (+) followed by FCeR1^{+} with CD117 (c-Kit^{+}) expression.

Intestines: Tissue-specific protocols were used to obtain single cells suspensions. Following the euthanasia by Avertin injection, small (ileum) and large (cecum and proximal colon) intestines were rapidly removed and placed in ice-cold PBS. The intestinal tissue was opened longitudinally after removal of fat and connective tissues. Fecal content was removed and the tissue was cut into pieces (approximately 1.0 cm) after washed in ice-cold PBS. Intestinal tissues were then incubated in 5 mL of 5 mM ethylenediaminetetraacetic acid (EDTA) in Hank's Buffered Salt Solution (HBSS, Invitrogen, Carlsbad, CA) for 30 min at 37 °C with slow rotation (100 rpm). The epithelial cell layer was removed and filtered through a 70 µm cell strainers. The retrieved intestinal pieces were washed in HBSS and cut into smaller pieces and immersed in 10 mL digestion solution containing 5% FBS (Sigma-Aldrich, St. Louis, MO), collagenase IV (1.75 mg/mL; Roche, Nutley), and DNase I (0.5 mg/mL; Sigma-Aldrich) at 37 °C for 45 min with slow rotation. MCs were gated for CD45 positive (+) followed by FCeR1^{+} with CD117 (c-Kit^{+}) expression.

Mass spectrometry histamine quantification:

Histamine concentrations were quantified in the blood plasma at 6 hours, 24 hours post-stroke and sham control of Yg and Ag mice. Blood plasma was processed through methanol (Sigma Aldrich, USA) separation. The obtained supernatants were transferred into 3-kDa filtrate and centrifuged for 14,000 g, 40 min at room temperature. Flow-through was collected and mass spectrometry analysis was performed. Mass spectrometric quantification was performed as follows,

Histamine, formic acid (FA), and perfluoroheptanoic acid (PFHA) were obtained from Sigma-Aldrich (St. Louis, MO). Histamine-α,α,β,β-d4 was obtained from CDN isotopes (Pointe-Claire, Canada). Water and acetonitrile (ACN) were obtained from Fisher Scientific (Waltham, MA). The histamine-d4 internal standard solution was prepared at a concentration of 250 ng/mL of d4-histamine in water with 0.1% FA. 30 µL of internal standard solution was added to 30 µL of each sample, vortexed for 1 min, and dried in a SpeedVac for 5 hours. 30 µL of water:0.1% FA was added to each sample, vortexed for 1 min and centrifuged for 5 min at 10,000 rpm. Samples were then loaded into 0.5 mL autosampler vials for quantification.

Chromatography was performed on a Shimadzu (Kyoto, Japan) Nexera-XR HPLC system consisting of a SIL-20ACxr autosampler, a CTO-20AC column oven and 2 LC-20ADxr binary pumps. Samples were loaded onto a Phenomenex (Torrance, CA) 1 mm x 50 mm phenylhexyl reversed-phased column equipped with a Phenomenex phenylhexyl 4 mm x 2 mm guard column. The aqueous mobile phase (A) consisted of

H_2O:ACN:FA:PFHA (99.3:0.5:0.1:0.1 v/v/v/v) and the organic mobile phase (B) consisted of H_2O:FA (99.9:0.1 v/v). Column flow was 80 µL/min and 5µL of sample was injected onto the column and eluted with a constant mobile phase flow rate of 80 µL/min. The elution gradient was optimized as follows: started from 10% B and increased to 70% B over 5 min; ramp to 80% B for 6 sec and held for 1min; ramp back to 10% B over 6 sec and maintained at 10% for a total chromatographic run time of 12 min to re-equilibrate.

Selected reaction monitoring (SRM) was performed on a Sciex (Framingham, MA) 6500 QTRAP with a Turbo V source. The mass spectrometer was operated in the positive ion mode under the following conditions: curtain gas: 20 psi; collision gas: HIGH; spray voltage: 4.5 kV; ion source gas 1: 20 psi; ion source gas 2: 20 psi; interface heater temperature: 175° C; Q1 and Q3 resolution: unit; scan time: 100 mS; de-clustering potential: 100 V; entrance potential: 8 V; collision exit potential: 10 V. The instrument was calibrated by using Sciex PPG calibration standard and tuned to the manufacturer's specifications. SRM transitions monitored for histamine were 112 → 95 (20eV) and 112 → 68 (30eV). For histamine-d4, the SRM transitions 116 → 99 (20eV) and 116 → 72 (30eV) were monitored. Data were acquired with Analyst® Software (ver 1.6.2) and quantification performed using Multiquant™ Software (ver 3.0.1).

Statistics:

Data were tested for normal distribution using the Kolmogorov–Smirnov test. Normally distributed data are presented as means with standard deviation while the medians with their range are given for non-normally distributed data. Significance of differences between Sham (control) and Stroke (experimental) at 6 hours, 24 hours and 7days post-stroke mice were analyzed using the One-way analysis of variance test for normally distributed data (or) the Kruskal-Wallis test for non-normally distributed data, followed by either Bonferroni /Tukey's multiple comparison post-hoc tests. Differences between sham and stroke at single time-point were analyzed using students t-test followed by the Mann-Whitney test for non-normally distributed data. Differences between the groups were considered significant at *$P < 0{\cdot}05$, **$P<0.01$, ***$p<0.001$. Prism 5.0 software (Graph Pad Software, Inc., La Jolla, CA, USA) for Windows, was used for data presentation and for data analysis. All experiments were performed by an investigator blinded to stroke and age groups during analysis. Differences in Phyla in the gut microbiota of young and aged mice were analyzed using the unweighted UniFrac distance and plotted in a Principal Coordinates Analysis. The UniFrac distance is a measure that takes into account the branch length shared by the young and aged microbiota when placed on a common phylogenetic tree[36, 37].

Results

Aging is associated with increased number of mast cells (MCs) in the gut and in the brain. Aging is an important risk factor for stroke and is accompanied by low-level inflammation [3, 38]. Aging alters the immunological response to stroke [38, 39]. We investigated if aging has an impact on tissue-specific MC populations and if age-associated differences in MCs play a role in post-stroke inflammation. MC progenitors are housed in the intestinal mucosa. Thus, we first investigated changes in the MC

populations in the gut and the brain of naïve Yg (3 months) and Ag (20 months) male WT mice. After exclusion of B cells, T cells, macrophages, and dendritic cells, MCs were identified as $CD45^+$ $FCeR1^+$ $CD117/c\text{-}Kit^+$ population. We found a significant increase in relative frequency of MCs, as a percentage of $CD45^+$ population, in both the gut and the brain of Ag mice compared to Yg mice (**Figure 1**). We then, using human brain samples, investigated the presence of MCs in the infarct area. Human brain autopsy samples from stroke patients showed highly granulated MCs around the infarct area whereas MCs were not detected in young or aged control samples (**Supplemental Figure 1**). We then determined if the increased number of gut MCs was associated with higher levels of circulating HA after stroke in Ag and Yg mice.

Stroke leads to elevated HA in the systemic circulation in an age dependent manner. HA is released by resident MCs, as an immediate response to tissue injury and initiator of inflammation [9, 12-17]. We hypothesized that aging leads to increases in systemic HA levels after stroke. We quantified plasma HA levels at 6 and 24 hours after stroke in Yg (3 months) and Ag (20 months) mice. Mass spectrometry analysis demonstrated that Yg mice showed no changes in plasma HA levels at 6 and 24 hours (*Yg: 6-h= 1.12±0.2 and 24-h= 1.10±0.18 ng* ml^{-1}*)* after stroke compared to age-matched sham controls. In contrast, Ag mice exhibited an increase in plasma HA levels at 6 hours that was significantly increased at 24 hours after stroke when compared to age-matched shams (**Figure 2A**). In line with these systemic changes, brain HA levels were significantly higher at 6 hours after stroke in Ag group when compared to age-matched shams (**Figure 2B**). This increased brain HA level was not significant at 24 hours, although there was a trend towards increased in HA levels after stroke in the Ag group (**Figure 2B**). No changes in brain HA level was observed in the Yg group at either timepoint (data not shown). These findings suggest that aging is associated with increased plasma and brain HA levels after stroke in the acute phase. We speculated that increased systemic HA levels after stroke might also lead to increased HA receptor expression in the gut.

Stroke leads to elevated gut mucosal H2R expression. We then determined whether this increase in systemic HA levels after stroke in Ag but not Yg mice is associated with increased expression of the gut-specific HA receptor, H2R in Ag but not in Yg mice after stroke. We performed mRNA gene expression analysis from gut tissues of Yg and Ag mice at 6- and 24-hour post-stroke timepoints. We found that H2R gene expression was significantly increased in the gut mucosa at 24 hours after stroke in Ag mice but not in Yg mice, when compared to age-matched shams (**Figure 3A**). Since we observed a significant increase in H2R expression at 24 hours post-stroke only in aged mice, we performed additional experiments in Ag mice to examine the sub-acute effects of stroke on H2R expression in the gut mucosa. Gut tissue was collected from Ag (20 months) sham and stroke groups at 7 days post-stroke (7d PS). Ag mice showed significantly increased H2R expression in the gut at both the protein and mRNA levels within the intestinal mucosa (**Figure 3B-C**). This increased expression was significant in the lamina mucosa where most of the immune cells reside in the gut tissue. RNA in-situ hybridization (**Figure 3C**) showed increased H2R mRNA expression in the lamina mucosa, which further supports the notion that there is an increase in H2R protein levels after stroke in the gut epithelium of Ag mice at 7 days PS.

Stroke-induced HA release is associated with increased pro-inflammatory cytokines in the both systemic circulation and the gut. IL-6 is a key pro-inflammatory molecule and mediates stroke-induced inflammation [40-42]. IL-6 increases MCs maturation[43] by inducing the FceR1 receptor on MCs [44-47] and by upregulating HA production. In young mice, we found increased levels of plasma IL-6 at 6 hours post-stroke that normalized by 24 hours, when compared to age-matched shams. In aged mice however, a significant increase in plasma IL-6 levels observed at 6 hours persisted up to 24 hours after stroke, when compared to age-matched shams (**Figure 4A**).

Our data showed that granulocyte colony-stimulating factor (G-CSF) was significantly increased in the plasma at 6 hours after stroke in both Yg and Ag mice compared to age-matched shams. However, there was a significant reduction is plasma G-CSF by 24 hours after stroke only in Yg but not in Ag mice, when compared to age-matched shams (**Figure 4B**).

In the gut, IL-6 and TNF-α gene expression levels were significantly higher at 6 hours and 24 hours post-stroke in Ag mice compared to age-matched controls (**Figure 4C&E**). This increase was not seen in Yg mice (**Figure 4C&E**). IFN-γ expression was significantly increased at 24 hours after stroke in Ag mice whereas Yg mice had no change in IFN-γ levels at either timepoints when each group was compared to their age-matched shams (**Figure 4D**). Interestingly, IL-6 mRNA levels were significantly elevated in the gut even at 7d after stroke in aged mice compared to the age-matched sham controls (**Figure 4F**). These findings support our hypothesis that increased HA and pro-inflammatory cytokines increases in both the plasma and in the gut of aged animals at 24 hours after stroke, when compared to young cohorts.

Stroke leads to increased number of gut MCs. MCs are a primary source of HA during acute inflammation. Mucosal MC progenitors constitutively home to the intestinal mucosa and are recruited, then mature, after inflammatory stimuli [20, 21]. To investigate the cause of increased H2R expression, we examined the number of gut MCs after stroke in aged mice. Using immunohistochemistry, we found that young mice show no detectible levels of gut MCs 24 hours after stroke (**Figure 5A**). However, a significant increase in gut MCs was seen at 24 hours after stroke in aged mice compared to age-matched shams (**Figure 5A**). An increase in the gut MCs, assessed by tryptase signal intensity, was also present 7-days after stroke in aged mice, when compared to age-matched shams (**Figure 5B**).

***Stroke is associated with reduction in mucus-secreting goblet cells in the gut*.** Mucus is secreted by the goblet cells of the gut epithelium and is highly glycosylated[48]. In the presence of inflammation, mucus fucosylation is significantly depleted [8, 49]. To follow up on our results showing increased gut inflammation in aged mice, we assessed the mucus barrier integrity by quantifying the amount of fucosylated mucin in aged mice. Our results from aged mice at 7d post-stroke showed a significant reduction in goblet cells filled with fucosylated mucus, when compared to shams (**Figure 6A**). Reduced mucus barrier integrity was also associated with increased bacterial breach observed by fluorescence in-situ hybridization of the gut mucosa (**Figure 6B**). These findings suggest that increased gut inflammation in aged mice is associated with a loss of gut barrier integrity, which might explain the persistence of post-stroke inflammation in aged animals.

Increased H2R and MCs after stroke are associated with dysbiosis of the gut microbiota. The composition of gut microbiota can be influenced by intestinal inflammation[50]. We performed 16S rRNA sequencing on gut contents to examine alternations in the microbial diversity caused by stroke-induced inflammation in the Yg and Ag mice at 6 hours, 24 hours and 7-d after stroke and compared these to age-matched sham controls. Consistent with the increased H2R expression levels and MCs in the gut, aged mice showed a shift in the beta-diversity or between-samples diversity, with weighted UniFrac distances by principal coordinate analysis (PCoA), as early as 24 hours after stroke compared to age-matched controls (**Figure 7A**). Interestingly, we observed an increase in Verrucomicrobiaceae family in aged mice at 24 hours after stroke compared to age-matched shams (**Figure 7B**). These changes were not seen at the earlier timepoint of 6 hours in aged or young (6 and 24 hours) stroke mice. The alpha-diversity, or within-sample diversity, was not different between sham and stroke mice 7d post-stroke (not shown). Upon visualization of beta-diversity, or between-samples diversity, with weighted UniFrac distances by PCoA, a significant clustering effect ($p = 0.006$) emerged along the PC1 axis (69.5% variation explained) in 7d post-stroke Ag mice luminal content compared to pre-stroke Ag mice **(Figure 7C**). Closer examination of 16S data at the order level showed a significant reduction of Clostridiales and an increase in Bacteroidales in the aged mice 7d post-stroke compared to pre-stroke mice **(Figure 7D**). Overall, our 16S data show that compositional differences in the gut microbiota exist as early as 24 hours after stroke and continued at 7 days after stroke in aged mice, when compared to non-stroke samples (**Figure 7C&D**).

Discussion

Histamine (HA) is an important signaling molecule secreted from resident MCs [8, 9] and is necessary for MC maturation [15]. MCs progenitors are housed in the gut mucosa and migrate to the site of inflammation upon activation [20, 21]. MCs are early responders, and are involved in the acute blood-brain barrier changes after cerebral ischemia and hemorrhage [51]. Therefore, we hypothesized that stroke would increase gut MCs activation, leading to an elevation in systemic HA levels and an increase in peripheral inflammation. Elevated MCs signaling is known to increase inflammation due to increased HA release and HR expression [8, 9]. Our results demonstrated that stroke leads to an increase in the gut MC population in aged mice as early as 6 hours post-stroke. HA is an important signaling molecule from resident MCs [8, 9]. Our data support the assumption that an increase in gut MCs leads to an increase in systemic HA and H2R expression levels after stroke in Ag mice. In line with the elevation in H2R expression, we found elevated IL-6 expression levels in the gut mucosa after stroke only in Ag mice. IL-6 is a pro-inflammatory molecule and mediates stroke-induced inflammation [40-42] and also increases MCs maturation [43]. IL-6 also upregulates histamine production and induces the FceR1 immunoglobulin receptor found on mast cells [44-47]. In addition, we found that mucus secreting fucosylated goblet cells were reduced after stroke in Ag mice. Fucosylation of mucus is a major determinant of a healthy gut and reduction in fucosylation is associated with gut inflammation [5, 8, 52, 53]. Of note, these changes were only examined in male mice, as estradiol induces partial release of MCs [54]. As the estrous cycle varies

every 4 days in young female mice [33] we focused these initial studies on male mice. Evaluation of aged females would add translational value to these findings in future experiments.

Histamine release is an immediate response from MCs after injury, and this triggers the production of a variety of pro-inflammatory molecules [9, 11-17]. Previous work has shown that an increase in systemic HA levels occurs with aging [31]. In association with altered HA levels, changes in IL-1β and TNFα in the brain have also been reported [55]. Similarly, we observed elevated HA levels in the brain of Ag mice acutely after stroke (6 hours) but not at the sub-acute timepoint of 24 hours. In contrast, post-stroke HA levels remain high at both acute and sub-acute phases in the plasma of Ag mice. We then investigated the role of the gut in the stroke-induced elevation of HA. Previous studies have shown that gut mucosal MCs (gMCs) are a major source of HA [18, 19]. Interestingly, mucosal MC progenitors constitutively home to the intestinal mucosa and are recruited and matured during inflammation [20, 21]. Importantly, our data showed a basal increase in resident MCs in the brain and gut of aged mice compared to young mice. Therefore, we believe that the increase in systemic HA induced by stroke is secondary to the increased gut MCs population in Ag mice. In support of this hypothesis, we observed a significant increase in the gut MCs at 24 hours after stroke and found this this effect to be age-dependent.

Reducing HA signaling may have therapeutic potential. Administration of a H2R antagonist was associated with preserved stroke volume and reduced risk for incident heart failure [56]. Others have found that administration of ranitidine, a H2-receptor antagonist, reduced neuronal death induced by oxygen-glucose deprivation in an *in vitro* model of ischemia [57]. In line with these observations, we found a significant increase in H2R expression in the gut as early as 24 hours and as late as 7-days after stroke in aged mice. Therefore, we speculate that stroke increases gut MCs, which contributes to severe peripheral inflammation via increased gut HA-H2R activation in Ag mice. In line with these findings, we found that pro-inflammatory cytokines, such as IL-6, TNF-α and IFN-γ were increased in the gut mucosa of aged mice after stroke. Similarly, we found increased systemic pro-inflammatory cytokines IL-6 and G-CSF levels in aged mice at both 6 hours and at 24 hours after stroke.

A previous study has reported that MCs derived from meninges worsen damage in murine models of stroke [30]. However, this study used global MC knockout mice, that had MCs deleted from all tissues. Therefore, the role of peripheral MCs, specifically those from the gut where most progenitor MCs are found, was not studied. This study is the first evidence that shows the importance of peripheral MCs and their role in stroke in aged animals. Our group has previously shown that stroke leads to increased neuroinflammation in aged animals [37, 38, 58]. We have also shown that the gut is “inflamed” after stroke [37]. However, the initial trigger that connects the brain-gut axis in the response to stroke is not understood. MCs are abundant in the gastrointestinal mucosa [21] and their activation is a primary response to tissue injury [59]. Stroke induces HA accumulation and causes MC degranulation in the neonatal brain [4]. Interestingly, MCs are also early responders in the regulation of acute blood-brain barrier changes after cerebral ischemia and hemorrhage [51] and likely play a key role in the response to injury. In keeping with our hypothesis, we observed an increase in gut MCs, gut H2R expression, and circulating HA levels after stroke with age. These changes were not seen in young mice after stroke,

reinforcing the value of examining aged mice in experimental stroke studies. This is important as stroke mainly affects older individuals [60]. We believe that the increase in gut MCs at the sub-acute phase of 24 hours might be an important link in the brain-gut axis and the response to stroke. Future studies to validate these findings with knockout mice are needed to confirm the role of HA and gMCs in post-stroke inflammation. In addition, previous research in our lab has shown changes in infarct volume in aged and young male mice 24-hours post-stroke. However, the increased infarct volume and neurological scores observed in young post-stroke mice showed reduced inflammation (measured by T-cells, monocytes and microglia activation) compared to aged post-stroke mice that showed reduced infarct volume with increased inflammation in the brain [61]. However, since MCs are immediate responders in the injured site, it is of importance to look at histamine levels and mast cell activation post-stroke. Primarily, aged MCs are known to be in an increased state of activation [32]. Changes seen in MCs and inflammation observed in the presented study are primarily due to aging effects of stroke.

Mucus is secreted by goblet cells of the gut epithelium and it is highly glycosylated[48]. In the presence of inflammation, mucus fucosylation is significantly depleted [8]. Increased inflammation causes reduced mucus synthesis [5, 8], allowing luminal bacteria to come in close contact with the gut epithelium triggering further inflammation [49]. The intestinal sections obtained from aged post-stroke male mice at 7-days showed significantly reduced mucus fucosylation in our study. Since we only found increased systemic and gut mucosal inflammation in aged mice at 24-hours, we assessed the mucus barrier integrity by quantifying the amount of fucosylated mucin only in aged mice at 7 days post-stroke to understand the persisting gut dysfunction long after stroke that might have potential impact on poorer stroke outcomes.

Our lab has previously demonstrated that gut dysbiosis (imbalanced microbiota composition leading to reduced barrier integrity [62]) plays an important role in the increased peripheral inflammation seen after stroke in aged animals [37]. Significant changes were seen up to 7 days after stroke in aged mice, but not in young mice, re-emphasizing the value of using aged animal models in stroke studies. Similar to the observation presented by *Wong et al* [25], the family Verrucomicrobiaceae was the dominant family in the gut of aged mice after stroke. Most bacterial species within this family belongs to *Akkermansia muciniphila*, a mucin degrader. *A. muciniphila* is known to contribute to gut inflammation[3]. This increase in mucin-degrading bacteria may be a link between the loss of protective mucus barrier that was seen after stroke. This work demonstrates that HA-HR levels are upregulated in the gut shortly after stroke and this is restricted to aged animals. Interestingly, human brain autopsy samples from stroke patients showed MC around the infarct area (**Supplemental Figure 1**). In addition, stroke and transient ischemic patients display significant changes in gut microbiota composition reported earlier independent of the co-morbidities. This might be due to the sudden severe pain and it is a known to cause poor bowel moments[63]. Reduction in bowel moments can indirectly induce dysbiotic microbiome[64]. However, inflammation is known to be the primary cause that leads to long-term health defects and dysbiosis might contributes to this pathological outcome.

Conclusion

Post-stroke inflammation is a critical determinant of damage and recovery after stroke[65]. HA secretion after MC degranulation may contribute to inflammation via activation of H2R, blood-brain-barrier disruption and recruitment of other immune cells to the ischemic brain. Our results show that the increase in gut MCs might be an innate immune response connecting the brain and gut after stroke. This study demonstrates that gut MCs and the H2R are upregulated after stroke in an age-dependent manner and are one of the primary events that occur following stroke. Our data highlight the importance of gut immune cells, specifically MCs in examining the peripheral response mediated by the brain-gut axis dysfunction after stroke.

Abbreviations

MC: mast cells

gMC: gut mast cells

HA: Histamine

HR2: Histamine receptor 2

MCAO: Middle cerebral artery occlusion

IL: Interleukin

TNF-α: Tumor necrosis factor alpha

IFN-γ: Interferon gamma

G-CSF: Granulocyte colony stimulating factor

OTU: Operational taxonomic units

Declarations

Availability of data and materials

The datasets supporting the conclusions of this article are included within the article and its additional files are available from the corresponding author on reasonable request.

Acknowledgements

Not applicable

Funding

This work was supported by the National Institutes of Health (National Institute for Diabetes and Digestive and Kidney Diseases)-funded Texas Medical Center Digestive Diseases Center (DK56338) DDC-TMC P30DK056338 to B.P.G) (NINDS NS094543 and NIA AG058463 to L.D.M).

AUTHOR CONTRIBUTIONS

BPG was involved in the study design, completion of all experiments, data analysis and interpretation, and manuscript preparation. MPBC contributed to execution of experiments and obtaining raw data together with BPG. AC performed all the strokes. HA was involved in the study design and sample collection. PH contributed to scientific discussion and manuscript preparation. AG, SA, JD, SV, AM, DD contributed to completion of experiments together with BPG. AH was involved in running mass spectrometry for histamine analysis. JK provided human autopsy brain sections. RB and LDM were involved in the study design, data interpretation and manuscript editing.

ETHICS DECLARATIONS

Ethics approval and consent to participate

All procedures were performed in accordance with NIH guidelines for the care and use of laboratory animals and were approved by the Institutional Animal care and use committee of the University of Texas Health Science Center Houston.

Consent for publication

Not applicable.

Competing interests

The authors declare that they have no competing interests.

References

1. Bentsen, L., et al., *Outcome and risk factors presented in old patients above 80 years of age versus younger patients after ischemic stroke.* J Stroke Cerebrovasc Dis, 2014. **23**(7): p. 1944-8.
2. Durgan, D.J., et al., *Examining the Role of the Microbiota-Gut-Brain Axis in Stroke.* Stroke, 2019. **50**(8): p. 2270-2277.
3. Furman, D., et al., *Chronic inflammation in the etiology of disease across the life span.* Nat Med, 2019. **25**(12): p. 1822-1832.
4. Biran, V., et al., *Stroke induces histamine accumulation and mast cell degranulation in the neonatal rat brain.* Brain Pathol, 2008. **18**(1): p. 1-9.
5. Ganesh, B.P., et al., *Commensal Akkermansia muciniphila exacerbates gut inflammation in Salmonella Typhimurium-infected gnotobiotic mice.* PLoS One, 2013. **8**(9): p. e74963.

6. Ganesh, B.P., et al., *Enterococcus faecium NCIMB 10415 does not protect interleukin-10 knock-out mice from chronic gut inflammation.* Benef Microbes, 2012. **3**(1): p. 43-50.
7. Ganesh, B.P. and J. Versalovic, *Luminal Conversion and Immunoregulation by Probiotics.* Front Pharmacol, 2015. **6**: p. 269.
8. Ganesh, B.P., et al., *Diacylglycerol kinase synthesized by commensal Lactobacillus reuteri diminishes protein kinase C phosphorylation and histamine-mediated signaling in the mammalian intestinal epithelium.* Mucosal Immunol, 2018. **11**(2): p. 380-393.
9. Dong, H., X. Zhang, and Y. Qian, *Mast cells and neuroinflammation.* Med Sci Monit Basic Res, 2014. **20**: p. 200-6.
10. Ganesh, B.P., et al., *Diacylglycerol kinase synthesized by commensal Lactobacillus reuteri diminishes protein kinase C phosphorylation and histamine-mediated signaling in the mammalian intestinal epithelium.* Mucosal immunology, 2018. **11**: p. 380-393.
11. Bulfone-Paus, S., et al., *Positive and Negative Signals in Mast Cell Activation.* Trends Immunol, 2017. **38**(9): p. 657-667.
12. Christy, A.L., et al., *Mast cell activation and neutrophil recruitment promotes early and robust inflammation in the meninges in EAE.* J Autoimmun, 2013. **42**: p. 50-61.
13. Jin, Y., A.J. Silverman, and S.J. Vannucci, *Mast cells are early responders after hypoxia-ischemia in immature rat brain.* Stroke, 2009. **40**(9): p. 3107-12.
14. Kempuraj, D., et al., *Mast Cell Activation in Brain Injury, Stress, and Post-traumatic Stress Disorder and Alzheimer's Disease Pathogenesis.* Front Neurosci, 2017. **11**: p. 703.
15. Nakazawa, S., et al., *Histamine synthesis is required for granule maturation in murine mast cells.* Eur J Immunol, 2014. **44**(1): p. 204-14.
16. Parsons, M.E. and C.R. Ganellin, *Histamine and its receptors.* Br J Pharmacol, 2006. **147 Suppl 1**: p. S127-35.
17. Strbian, D., et al., *Mast cell stabilization reduces hemorrhage formation and mortality after administration of thrombolytics in experimental ischemic stroke.* Circulation, 2007. **116**(4): p. 411-8.
18. De Winter, B.Y., R.M. van den Wijngaard, and W.J. de Jonge, *Intestinal mast cells in gut inflammation and motility disturbances.* Biochim Biophys Acta, 2012. **1822**(1): p. 66-73.
19. Bieganski, T., et al., *Distribution and properties of human intestinal diamine oxidase and its relevance for the histamine catabolism.* Biochim Biophys Acta, 1983. **756**(2): p. 196-203.
20. Dwyer, D.F., et al., *Expression profiling of constitutive mast cells reveals a unique identity within the immune system.* Nat Immunol, 2016. **17**(7): p. 878-87.
21. Hallgren, J. and M.F. Gurish, *Mast cell progenitor trafficking and maturation.* Adv Exp Med Biol, 2011. **716**: p. 14-28.
22. Tuttolomondo, A., et al., *Immuno-inflammatory and thrombotic/fibrinolytic variables associated with acute ischemic stroke diagnosis.* Atherosclerosis, 2009. **203**(2): p. 503-8.

23. Albanese, A., et al., *Spontaneous chronic subdural hematomas in young adults with a deficiency in coagulation factor XIII. Report of three cases.* J Neurosurg, 2005. **102**(6): p. 1130-2.
24. Anrather, J. and C. Iadecola, *Inflammation and Stroke: An Overview.* Neurotherapeutics, 2016. **13**(4): p. 661-670.
25. Stanley, D., R.J. Moore, and C.H.Y. Wong, *An insight into intestinal mucosal microbiota disruption after stroke.* Sci Rep, 2018. **8**(1): p. 568.
26. Crapser, J., et al., *Ischemic stroke induces gut permeability and enhances bacterial translocation leading to sepsis in aged mice.* Aging (Albany NY), 2016. **8**(5): p. 1049-63.
27. Thangam, E.B., et al., *The Role of Histamine and Histamine Receptors in Mast Cell-Mediated Allergy and Inflammation: The Hunt for New Therapeutic Targets.* Front Immunol, 2018. **9**: p. 1873.
28. Sander, L.E., et al., *Selective expression of histamine receptors H1R, H2R, and H4R, but not H3R, in the human intestinal tract.* Gut, 2006. **55**(4): p. 498-504.
29. Lieberman, P., *The basics of histamine biology.* Ann Allergy Asthma Immunol, 2011. **106**(2 Suppl): p. S2-5.
30. Arac, A., et al., *Evidence that meningeal mast cells can worsen stroke pathology in mice.* Am J Pathol, 2014. **184**(9): p. 2493-504.
31. Maintz, L. and N. Novak, *Histamine and histamine intolerance.* Am J Clin Nutr, 2007. **85**(5): p. 1185-96.
32. Chatterjee, V. and A.A. Gashev, *Aging-associated shifts in functional status of mast cells located by adult and aged mesenteric lymphatic vessels.* Am J Physiol Heart Circ Physiol, 2012. **303**(6): p. H693-702.
33. Kim, H., et al., *Effects of the Female Estrous Cycle on the Sexual Behaviors and Ultrasonic Vocalizations of Male C57BL/6 and Autistic BTBR T+ tf/J Mice.* Exp Neurobiol, 2016. **25**(4): p. 156-62.
34. Engevik, M.A., et al., *Acidic conditions in the NHE2(-/-) mouse intestine result in an altered mucosa-associated bacterial population with changes in mucus oligosaccharides.* Cell Physiol Biochem, 2013. **32**(7): p. 111-28.
35. Ganesh, B.P., et al., *Enterococcus faecium NCIMB 10415 does not protect interleukin-10 knock-out mice from chronic gut inflammation.* Beneficial Microbes, 2012. **3**(1): p. 43-50.
36. Hollister, E.B., et al., *Structure and function of the healthy pre-adolescent pediatric gut microbiome.* Microbiome, 2015. **3**: p. 36.
37. Spychala, M.S., et al., *Age-related changes in the gut microbiota influence systemic inflammation and stroke outcome.* Ann Neurol, 2018.
38. Ritzel, R.M., et al., *Aging alters the immunological response to ischemic stroke.* Acta Neuropathol, 2018. **136**(1): p. 89-110.
39. Ritzel, R.M., et al., *Age-Associated Resident Memory CD8 T Cells in the Central Nervous System Are Primed To Potentiate Inflammation after Ischemic Brain Injury.* J Immunol, 2016. **196**(8): p. 3318-30.

40. Gabay, C., *Interleukin-6 and chronic inflammation.* Arthritis Res Ther, 2006. **8 Suppl 2**: p. S3.
41. McCarty, M.F., *Interleukin-6 as a central mediator of cardiovascular risk associated with chronic inflammation, smoking, diabetes, and visceral obesity: down-regulation with essential fatty acids, ethanol and pentoxifylline.* Med Hypotheses, 1999. **52**(5): p. 465-77.
42. Scheller, J., N. Ohnesorge, and S. Rose-John, *Interleukin-6 trans-signalling in chronic inflammation and cancer.* Scand J Immunol, 2006. **63**(5): p. 321-9.
43. Desai, A., et al., *IL-6 promotes an increase in human mast cell numbers and reactivity through suppression of suppressor of cytokine signaling 3.* J Allergy Clin Immunol, 2016. **137**(6): p. 1863-1871 e6.
44. Conti, P., et al., *Interleukin-6 and mast cells.* Allergy Asthma Proc, 2002. **23**(5): p. 331-5.
45. Kinoshita, T., et al., *Interleukin-6 directly modulates stem cell factor-dependent development of human mast cells derived from CD34(+) cord blood cells.* Blood, 1999. **94**(2): p. 496-508.
46. McHale, C., et al., *Interleukin-6 potentiates FcepsilonRI-induced PGD2 biosynthesis and induces VEGF from human in situ-matured skin mast cells.* Biochim Biophys Acta, 2018. **1862**(5): p. 1069-1078.
47. Nechushtan, H., et al., *Inhibition of degranulation and interleukin-6 production in mast cells derived from mice deficient in protein kinase Cbeta.* Blood, 2000. **95**(5): p. 1752-7.
48. Johansson, M.E. and G.C. Hansson, *Mucus and the goblet cell.* Dig Dis, 2013. **31**(3-4): p. 305-9.
49. Pelaseyed, T., et al., *The mucus and mucins of the goblet cells and enterocytes provide the first defense line of the gastrointestinal tract and interact with the immune system.* Immunol Rev, 2014. **260**(1): p. 8-20.
50. Shi, N., et al., *Interaction between the gut microbiome and mucosal immune system.* Mil Med Res, 2017. **4**: p. 14.
51. Lindsberg, P.J., D. Strbian, and M.L. Karjalainen-Lindsberg, *Mast cells as early responders in the regulation of acute blood-brain barrier changes after cerebral ischemia and hemorrhage.* J Cereb Blood Flow Metab, 2010. **30**(4): p. 689-702.
52. Gao, C., et al., *Histamine H2 Receptor-Mediated Suppression of Intestinal Inflammation by Probiotic Lactobacillus reuteri.* MBio, 2015. **6**(6): p. e01358-15.
53. Cornick, S., A. Tawiah, and K. Chadee, *Roles and regulation of the mucus barrier in the gut.* Tissue Barriers, 2015. **3**(1-2): p. e982426.
54. Zaitsu, M., et al., *Estradiol activates mast cells via a non-genomic estrogen receptor-alpha and calcium influx.* Mol Immunol, 2007. **44**(8): p. 1977-85.
55. Cacabelos, R., et al., *Histamine and Immune Biomarkers in CNS Disorders.* Mediators Inflamm, 2016. **2016**: p. 1924603.
56. Leary, P.J., et al., *Histamine H2 Receptor Antagonists, Left Ventricular Morphology, and Heart Failure Risk: The MESA Study.* J Am Coll Cardiol, 2016. **67**(13): p. 1544-1552.
57. Malagelada, C., et al., *Histamine H2-receptor antagonist ranitidine protects against neural death induced by oxygen-glucose deprivation.* Stroke, 2004. **35**(10): p. 2396-401.

58. Chauhan, A., et al., *Myeloid-specific TAK1 deletion results in reduced brain monocyte infiltration and improved outcomes after stroke.* J Neuroinflammation, 2018. **15**(1): p. 148.
59. Galli, S.J., M. Maurer, and C.S. Lantz, *Mast cells as sentinels of innate immunity.* Curr Opin Immunol, 1999. **11**(1): p. 53-9.
60. Benjamin, E.J., et al., *Heart Disease and Stroke Statistics-2019 Update: A Report From the American Heart Association.* Circulation, 2019. **139**(10): p. e56-e528.
61. Manwani, B., et al., *Differential effects of aging and sex on stroke induced inflammation across the lifespan.* Exp Neurol, 2013. **249**: p. 120-31.
62. Turner, J.R., *Intestinal mucosal barrier function in health and disease.* Nat Rev Immunol, 2009. **9**(11): p. 799-809.
63. Barletta, J.F., *Clinical and economic burden of opioid use for postsurgical pain: focus on ventilatory impairment and ileus.* Pharmacotherapy, 2012. **32**(9 Suppl): p. 12S-8S.
64. Ohkusa, T., et al., *Gut Microbiota and Chronic Constipation: A Review and Update.* Front Med (Lausanne), 2019. **6**: p. 19.
65. Broughton, B.R., et al., *Post-stroke inflammation and the potential efficacy of novel stem cell therapies: focus on amnion epithelial cells.* Front Cell Neurosci, 2012. **6**: p. 66.

Supplemental Figure Legend

Supplemental Figure 1: Visualization of mast cells (MC) by Toluidine blue staining in the infarct area of human autopsy aged stroke brain samples compared to young and age matched controls. Red arrow indicate mast cells in purple stain. (B) Information about human autopsy samples on age, sex, stroke age and MCs found.

Figures

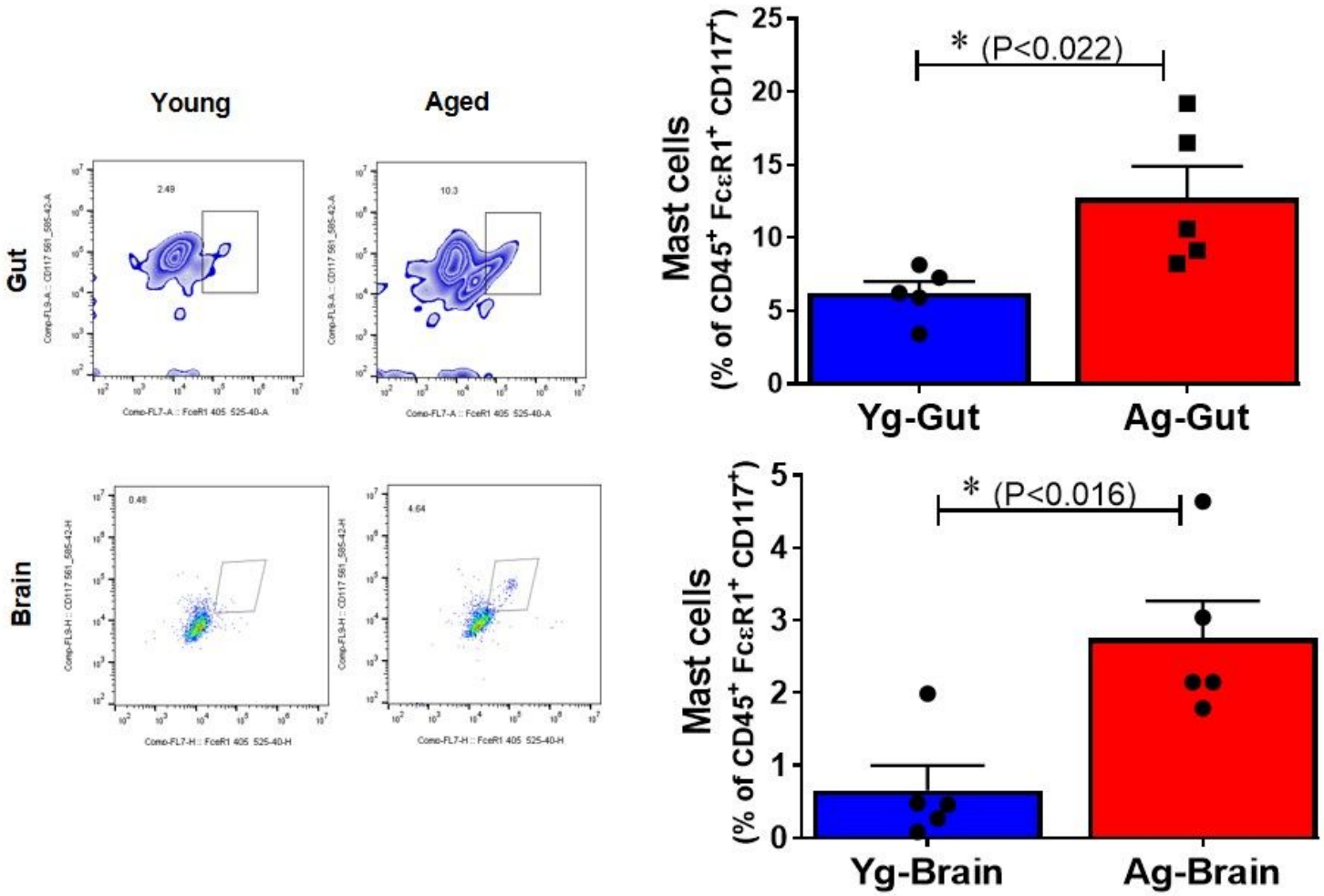

Figure 1

Aging caused two-fold increase in resident MC numbers in both gut and brain of aged compared to young mice. n=5 per group. Data are expressed as mean ± SEM, as well as individual values, and are obtained from two independent experiments at different time points. *p<0.05, **p<0.01. P values were calculated using two-tailed unpaired students t-test.

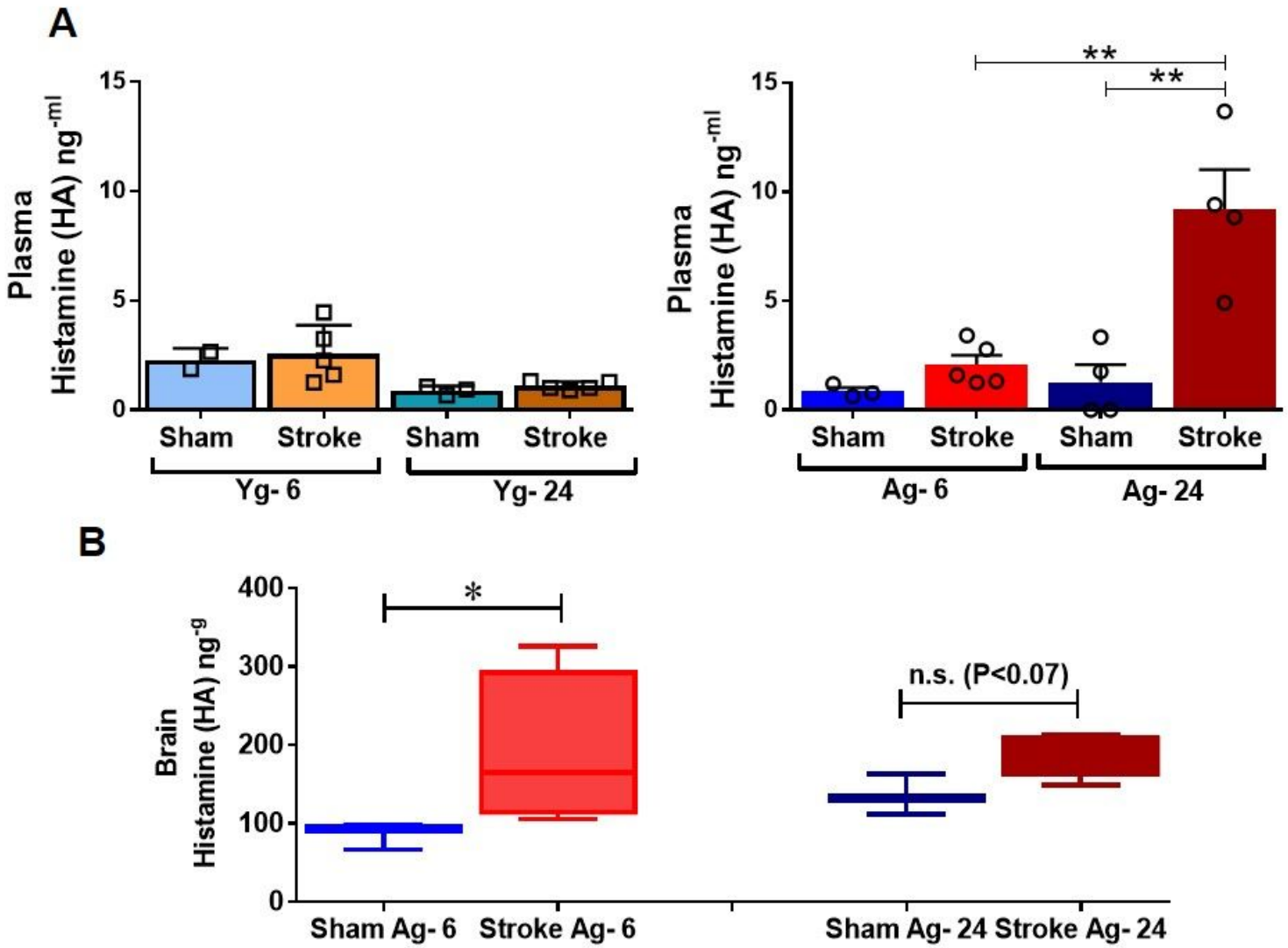

Figure 2

Elevated levels of histamine following ischemic stroke in (A) blood plasma of young (Yg) and aged (Ag) mice at 6 and 24 hours post-stroke compared to age matched controls. (B) Histamine levels of brain quantified by mass spectrometry in aged (Ag) mice at 6 and 24 hours post-stroke compared to age matched sham control mice. n=3 (sham) and 5(stroke) per group. Data are expressed as mean ± SEM (A) and median ± range (B), as well as individual values. *p<0.05, **p<0.01, ***p<0.001. P values were calculated using One-Way analysis of variance with Tukey multiple comparisons correction (A) and Kruskal-Wallis test with Dunn's multiple comparison (B).

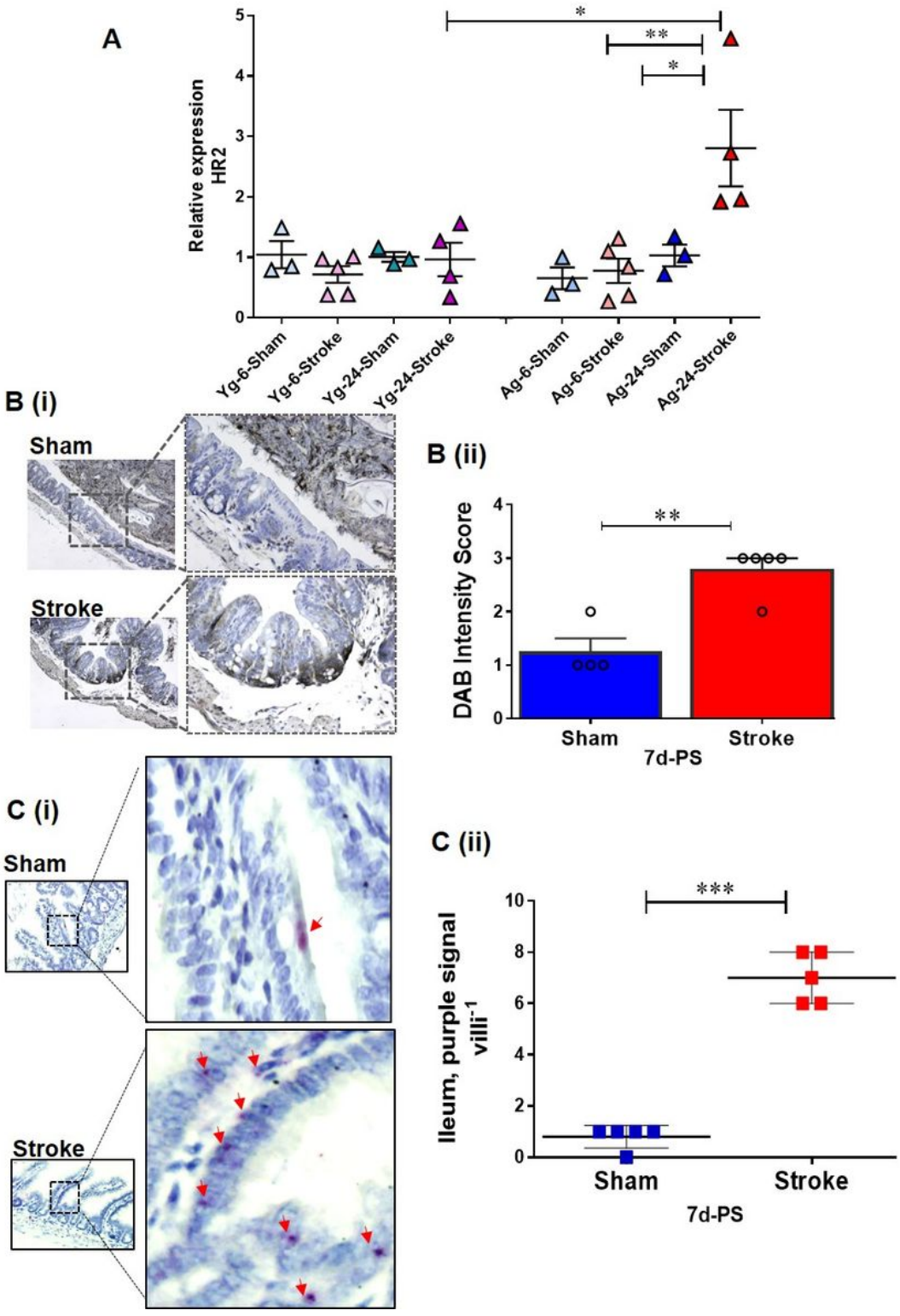

Figure 3

Increased levels of histamine receptor 2 (HR2) measured in the intestinal samples of young and aged mice for 6 hours, 24 hours and 7-days post-stroke compared to the age matched controls. A) mRNA expression levels of HR2 quantified by qPCR in young and aged mice at 6 and 24 hours post-stroke. B(i) Protein levels of HR2 quantified by IHC followed by image J quantification in aged mice at 7-days post-stroke and C) mRNA levels of HR2 quantified by RNA in-situ hybridization and analyzed by image-J in the

intestine of Ag mice at 7-days post-stroke . n=3 (sham) and 5 (stroke) per group (A) and 5 (sham) and 5 (stroke) per group (B&C). Data are expressed as mean ± SEM (A), (B) and (C), as well as individual values. *p<0.05, **p<0.01, ***p<0.001. P values were calculated using One-Way analysis of variance with Tukey multiple comparisons correction (A) or with two-tailed unpaired students t-test (B and C). (B) Brown-HR2 protein; blue-Nuclei (B) purple dots (red arrows)-mRNA HR2.

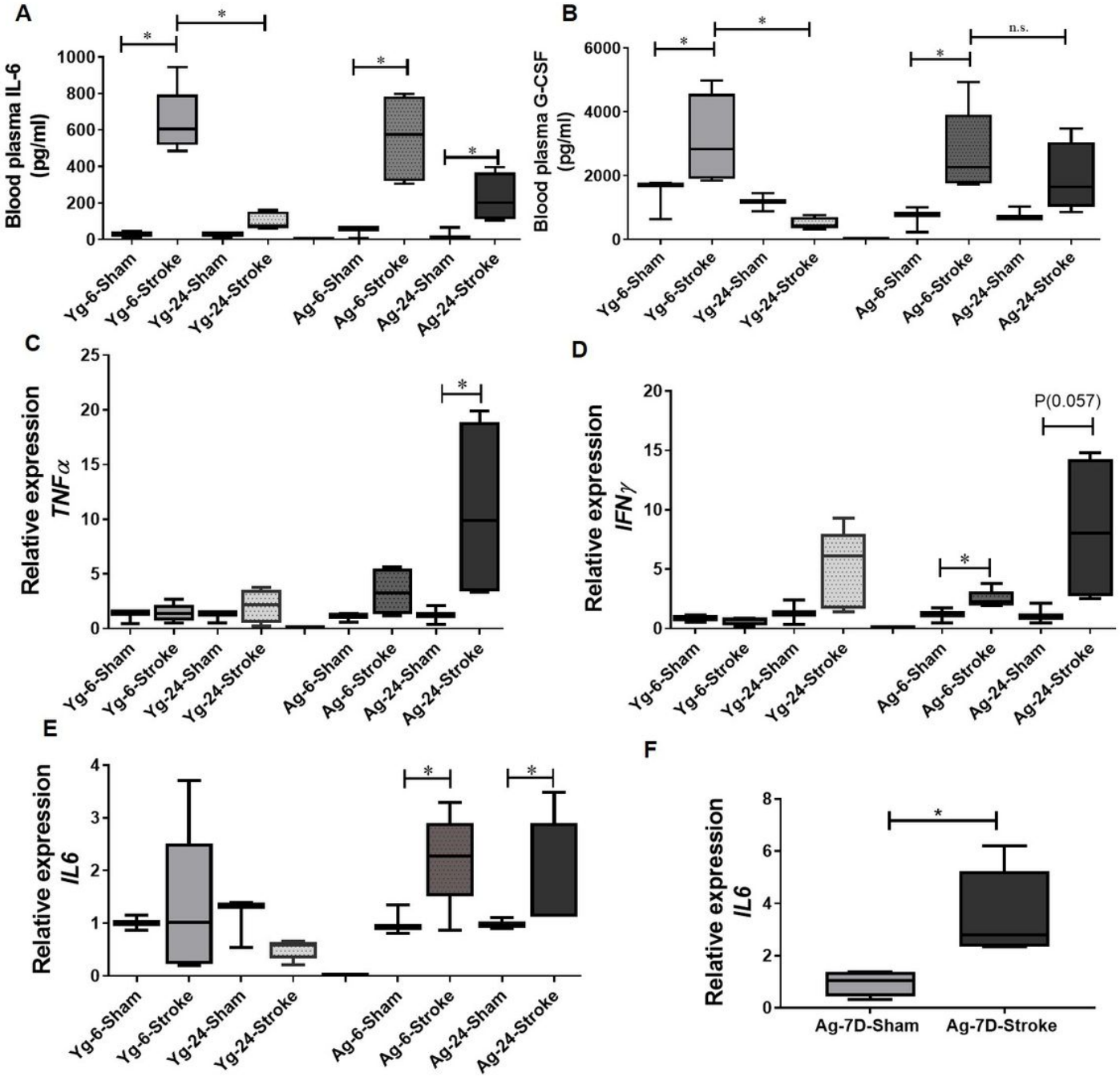

Figure 4

Elevated levels of inflammatory cytokines in the peripheral circulation and gut tissue of young and aged mice at 6 hours, 24 hours and 7-days post-stroke compared to the age matched sham controls. plasma levels of (A) IL-6 and (B) G-CSF quantified by multiplex at 6 hours and 24 hours post-stroke in young (Yg)

and aged (Ag) mice compared to sham controls. mRNA expression levels of pro-inflammatory cytokines (C) TNF-α, (D) IFN-γ, (E) IL-6 of gut tissue from Yg and Ag mice at 6 and 24 hours post-stroke compared to sham controls. (F) mRNA levels of IL-6 in gut tissue of aged mice at 7-days after stroke compared to aged matched sham controls. n=3 (sham) and 5 (stroke) per group (A-E) and 5 (sham) and 5 (stroke) per group (F). Data are expressed as median with range, as well as individual values. *P<0.05, **P<0.01, and ***P<0.001. P values were calculated using One-Way analysis of variance with Tukey multiple comparisons correction (A-E) and two-tailed unpaired students t-test, Mann-Whitney correction (F).

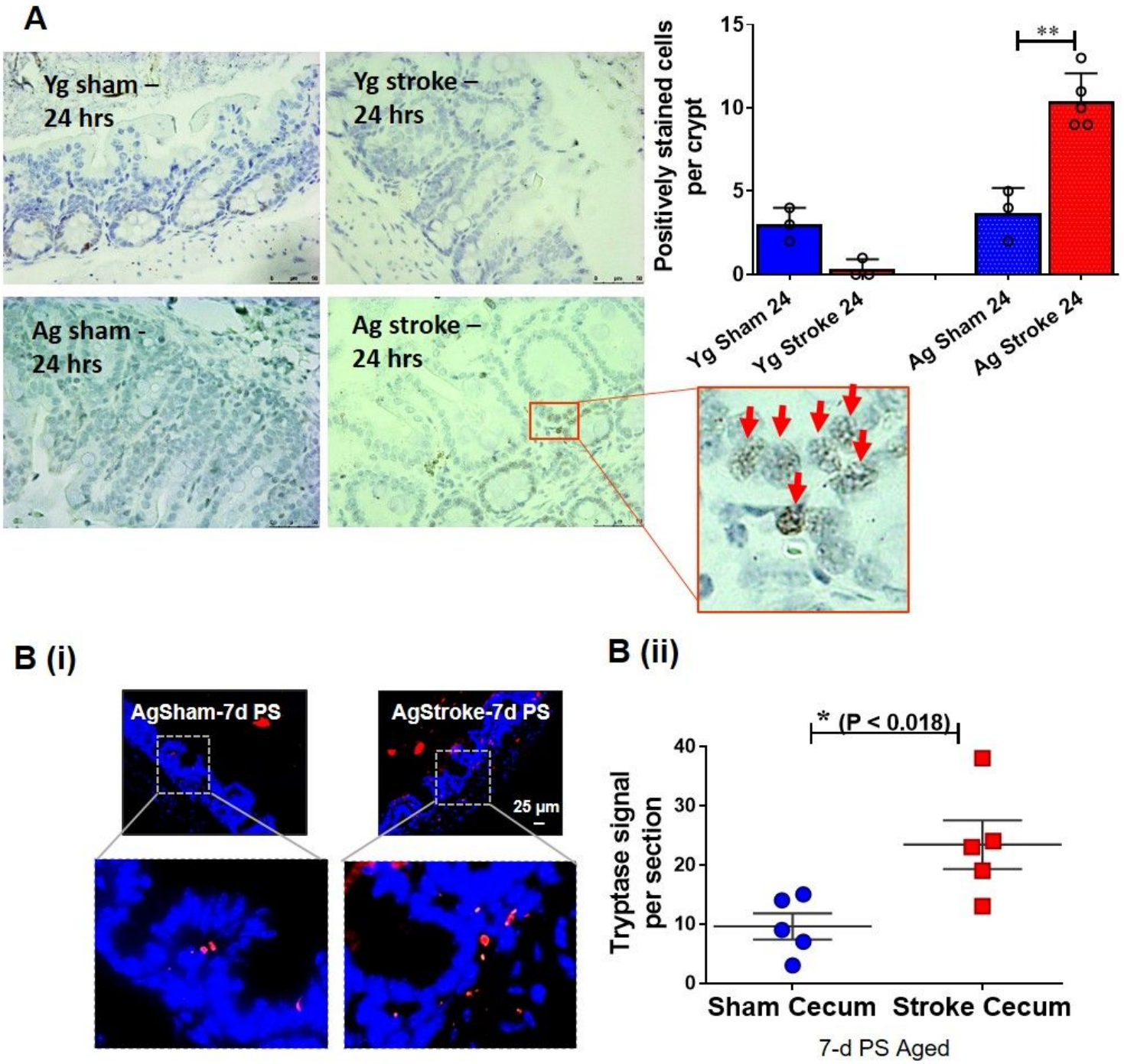

Figure 5

Increased mast cells (MC) numbers in the gut mucosa measured in the intestinal samples of young and aged mice for 6 hours, 24 hours and 7-days post-stroke compared to the age matched controls. (A) MCs quantified by immunohistochemistry in the intestinal samples of young and aged mice at 6 hours and 24 hours post-stroke compared to their age-matched sham controls. (B) MCs quantified by fluorescence immunohistochemistry in the intestinal samples of aged mice at 7-days post-stroke and C) mRNA levels of HR2 quantified by RNA in-situ hybridization and analyzed by image-J in the intestine of Ag mice at 7-days post-stroke . n=3 (sham) and 5 (stroke) per group (A) and 5 (sham) and 5 (stroke) per group (B). Data are expressed as mean ± SEM (A) and (B), as well as individual values. *p<0.05, **p<0.01, ***p<0.001. P values were calculated using One-Way analysis of variance with Tukey multiple comparisons correction (A) and two-tailed unpaired students t-test (B). (A) Red arrows-Mast cell; (B) Red-mast cells.

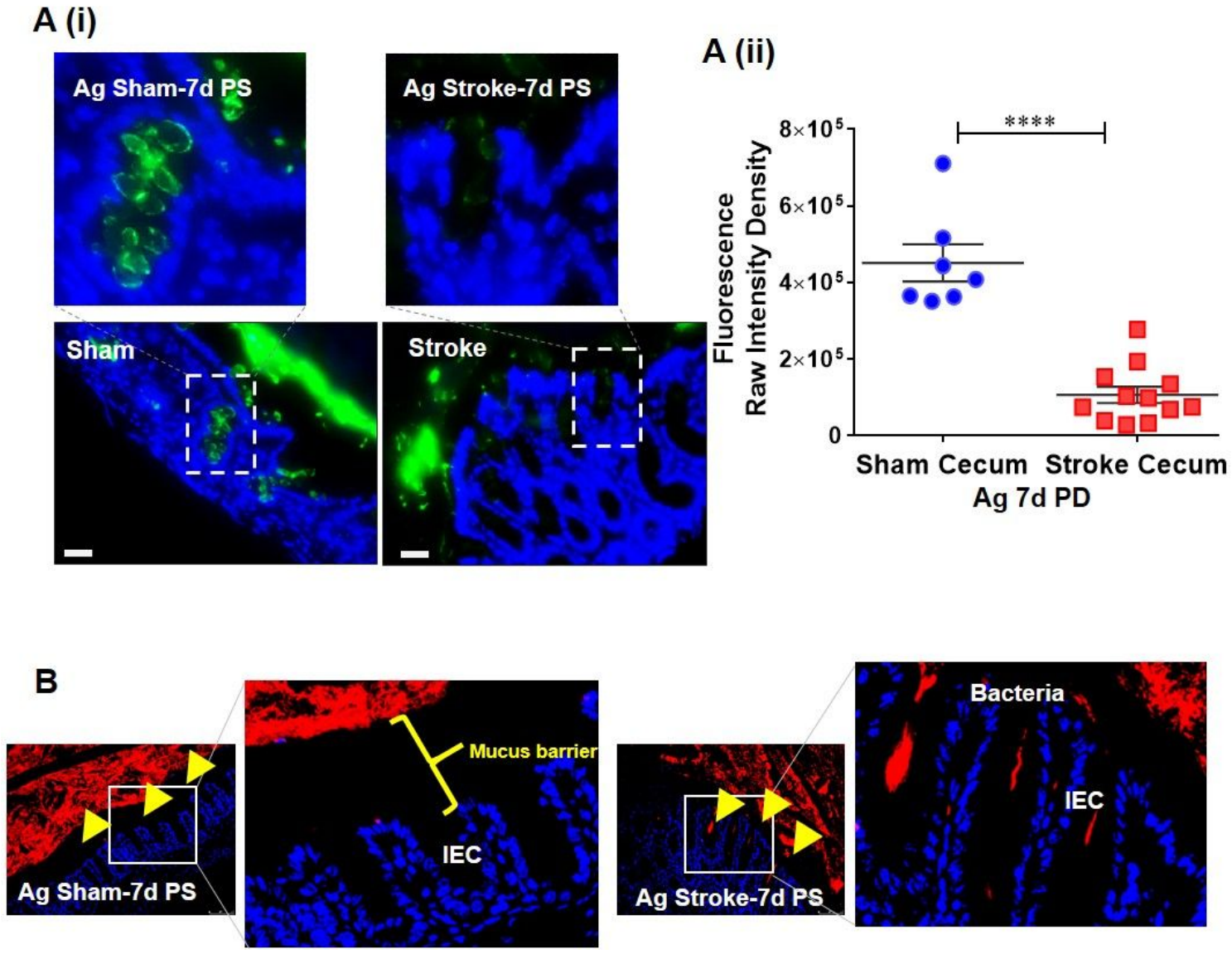

Figure 6

Reduced Fucosylated goblet cells and mucus barrier of the gut mucosa measured in the intestinal samples of aged mice 7-days post-stroke compared to the age matched controls. (A) Goblet cells

analyzed by immunohistochemistry and quantified by image-J in the intestinal samples of aged mice at 7-days post-stroke compared to their age-matched sham controls. (B) FISH staining showing bacterial growth and mucus thickness of gut tissue measured by confocal microscopy in the intestinal samples of aged mice at 7-days post-stroke. Number of mice used 5 (sham) and 5 (stroke) per group (A&B). Data are expressed as mean ± SEM (A) as well as individual values. *p<0.05, **p<0.01, ***p<0.001. P values were calculated using two-tailed unpaired students t-test. (A) Green-fucosylated goblet cell and mucus; (B) red-Bacterial biofilm (A&B) Blue-DAPI nuclei stain.

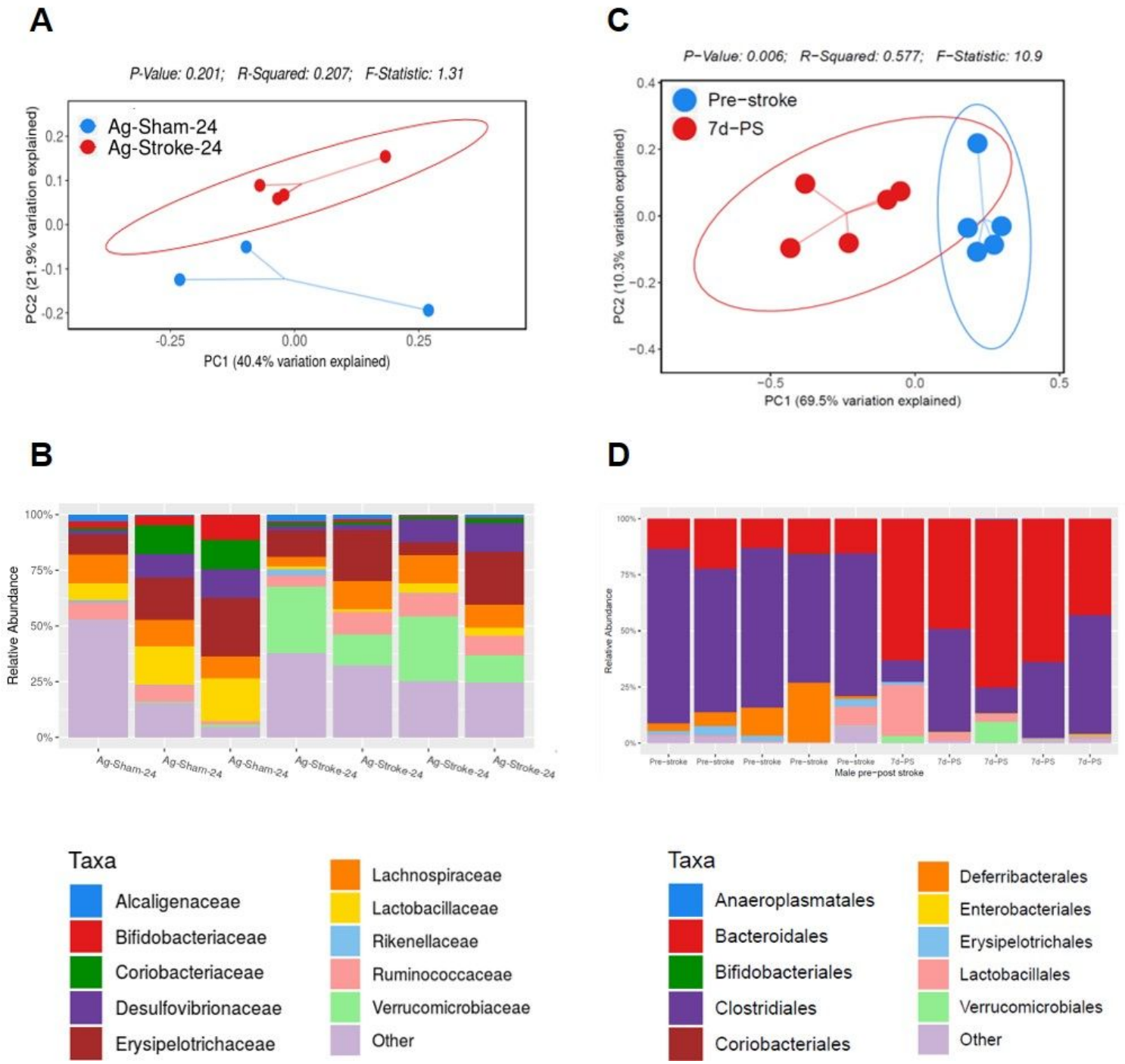

Figure 7

Compositional differences in gut microbiota by 16S rRNA sequencing and qPCR of intestinal luminal content. (A) visualization of beta-diversity, or between-samples diversity, with weighted UniFrac distances by principal coordinate analysis (PCoA) shows a clustering effect by strain between aged mice at 24 hours post-stroke compared to age matched sham controls and (B) corresponding family level bacterial distribution. (C) visualization of beta-diversity, or between-samples diversity, with weighted UniFrac distances by principal coordinate analysis (PCoA) shows a clustering effect by strain between aged mice at 7-days post-stroke compared to age matched sham controls and (D) corresponding order level bacterial distribution. n=3 sham and n=5 stroke (A&B); n=5 sham and n=5 stroke (C&D).

Supplementary Files

This is a list of supplementary files associated with this preprint. Click to download.

- SupplementalFigure1.jpg